THE FEATURES OF SPORTS COMPLEX 'SUNKAR' MONITORING BY TERRESTRIAL LASER SCANNING

R. Shults [1], G. Seitkazina [2], S. Soltabayeva [3]

[1] King Fahd University of Petroleum & Minerals, IRC for Aviation and Space Exploration, Dhahran 31261, Kingdom of Saudi Arabia - roman.shults@kfupm.edu.sa

[2] Shakarim University, Semey, 071412 Republic of Kazakhstan – s_gulnura_s@mail.ru

[3] Satbayev University, Almaty, 050013, Republic of Kazakhstan - s.soltabayeva@satbayev.university

KEY WORDS: Terrestrial laser scanning, Monitoring, Displacement, Longitudinal axis, Spline.

ABSTRACT:

The paper is aimed at the study of monitoring workflow in adverse observation conditions for sports structures. The application of terrestrial laser scanning for monitoring various objects is well-studied. However, the deployment of TLS for large sports structures is challenging. Such structures have huge sizes, complex geometry and need the control of particular elements. The monitoring gets complicated in the case when the structure is placed on a very steep slope, e.g., ski jumps or bobsleigh tracks. The subject of the presented study is the complex of ski jumps 'Sunkar' emplaced in Almaty, Republic of Kazakhstan. The monitoring network for the complex was created using a robotic total station. Due to the extreme sizes of the object (height 70 m, width 8 m, length over 100 m), TLS was accomplished from all points of the network to ensure the necessary density of point clouds and reliable georeferencing. The main observation parameters were the displacements of the ski jumps regarding the longitudinal axis. To retrieve the axis coordinates, the point cloud was sliced along the ski jump surface. The geometry of the longitudinal axis was simulated using spline functions. As an output, the suggested monitoring workflow is provided that ensures the quality of the necessary results.

1. INTRODUCTION

Terrestrial laser scanning (TLS) plays an essential role in the tasks of geospatial monitoring of engineering structures. The main advantage of TLS is high data redundancy. Such redundancy allows the detailed modeling of different structure elements (Vezočnik et al. 2009). By comparing simulated point clouds, one may detect the deformed regions and the total displacement of the structure from its initial position (Holst et al. 2017). TLS has been successfully studied and applied for various monitoring problems in recent years. Numerous scholars have stressed the importance of TLS for monitoring bridges (Cha et al. 2017, Rashidi et al. 2021), cooling towers (Ioannidis et al. 2006), hydro-technical objects (Schäfer et al. 2004, Schneider 2006, Koska et al. 2008), tunnels (Lindenbergh et al. 2005, Nuttens et al. 2010, Xu et al. 2019), structural elements testing (Nguyen and Weinand, 2020), pipelines (Qiu and Wu, 2008, Shults et al. 2022), historical buildings (Sternberg 2006, Shults et al. 2017), open pit mines (Tong et al. 2015), etc. The development of the total stations with scanning options has extended the opportunities of TLS. The surveyors have obtained an opportunity to create a monitoring network and scan the object using the same device simultaneously. On the other hand, the progress in software development has allowed the processing of vast amounts of data and output of any necessary results, e.g., models (solid, wireframes, points), meshes, drawings, cross-sections, point clouds, and much more. These achievements have created premises for extended applications of TLS monitoring almost to any engineering structure. Among those structures, sports structures take an essential role. These structures have a pretty sophisticated geometry and large sizes and often are emplaced in regions with complex geological conditions. These circumstances are pertinent for such structures as ski jumps. Ski jumps always build up in mountainous regions that are characterized by very severe geological conditions and are subjected to landslide processes and adverse weather conditions. The paper presents the case study of ski jump monitoring using the scanning total station, monitoring results, and the technical workflow of the monitoring.

2. MONITORING OBJECT

The study object is the Sunkar International Ski Jumping Complex located in the southern part of Almaty, Republic of Kazakhstan, at a height of 900 m above sea level. The complex consists of five ski jumps. The longest one is K125, length 125 m. The neighboring ski jump is K95 and has a length of 95 m. Those two ski jumps (Figure 1) have been selected for detailed monitoring.

Figure 1. Ski jumps K125 and K90.

Figure 2. The ramp of the ski jump K125.

The geometry of ski jumps is pretty complex (Figure 2). The curved ramp is made of steel trusses overlaid by a concrete runway and covered hill for landing. In general, the ramp presents a geometrical curve resembling a parabola. However, in reality, the geometry is more complex. One may see that the complex is located in regions prone to landslide activity. During the year, the sports complex undergoes serious loads of snowfalls and wind gusts. Another factor is the seismicity of the Almaty city. For years this region has been subjected to permanent earthquakes, some of which had disastrous effects, e.g., in 1911, 1936, 1967, and 1971. Those earthquakes had brought about many landslides. Summing up, the sports complex is affected by various environmental factors. These conditions dictate the necessity of geospatial monitoring of the sports complex.

3. MONITORING

3.1 Monitoring Workflow

The starting point of any monitoring project is the development of a monitoring workflow that is presented in the form of a flowchart. For this specific object, the monitoring flowchart has been developed (Figure 3). The flowchart contains three main blocks presenting the design step, fieldwork and processing/modeling step, and the results delivered. The design step supposes the various accuracy calculations, establishing scanning stations, choosing the equipment, point foundation, target preparation, and emplacement. The scanner check/calibration before the fieldwork is essential to ensure that it provides the necessary accuracy, being that any monitoring task requires high measurement accuracy.

The fieldworks begin with the network creation and coordinating the targets for further cloud georeferencing. The network creation follows the scanning step. This step actually takes up to 10% of the working time for the whole project. Thanks to the total station with the scanning function, network creation, and scanning are possible with the same equipment. The data after point cloud acquisition go to processing. The processing is the most time-consuming stage. The separate point clouds are referenced during the processing into one point cloud model defined in the common coordinate system. Upon the finishing of georeferencing, the point cloud is triangulated, meshed, and, if necessary, modeled.

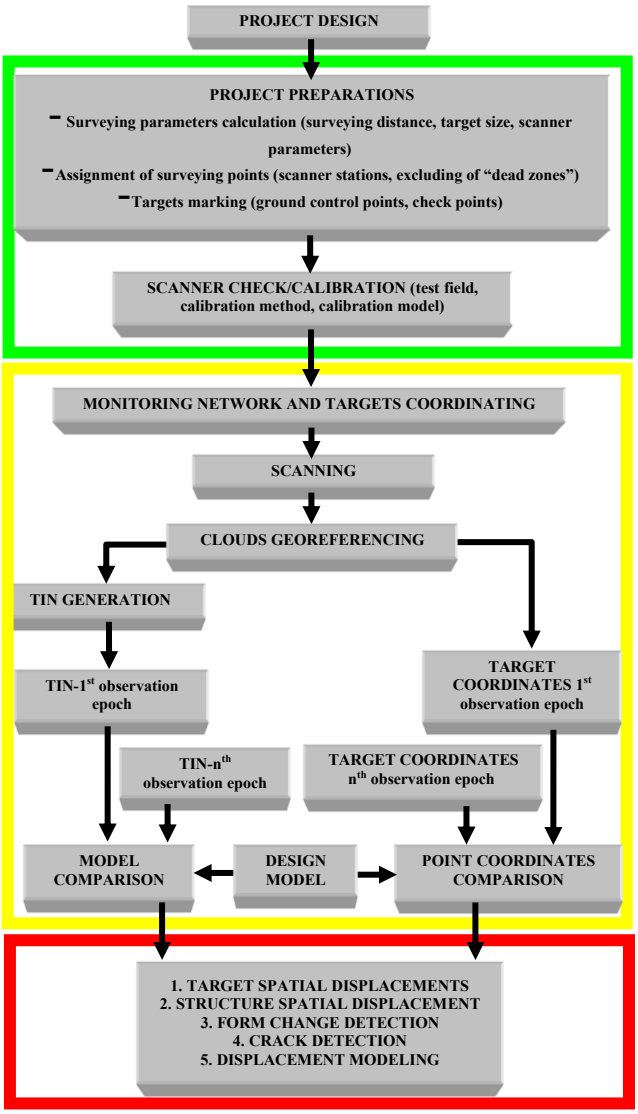

Figure 3. Monitoring flowchart.

The comparison step finishes the processing stage. The comparison is possible in different ways. The simplest case is the comparison of reference target coordinates. However, in this case, the approach has no difference from ordinary total station surveying. Much more informative is the comparison between TIN models from different observation epochs. This comparison provides a whole picture of the structure deformation. Except for comparing different TIN models, for the relatively new structures, it is possible to equalize the scanning results with the existing design model.

The final step is the results reporting. The comparison output may present spatial displacements of specific points (targets), the structure displacement in total, the changes of the structure deformation (geometry changes), possible crack detection, and prediction models for displacement evolution. The forecasting models are built up based on several observation epochs and may include different observation parameters, such as volume of precipitation, temperature variation, groundwater level, etc., for the case of the given object, of interest are vertical displacements along the longitude axis of the ramp. Thus, the appropriate processing method has been suggested and considered in Section 4.

3.2 Monitoring Network

The observation network has been created using scanning total station Leica Nova MS60. The geometry of the sports complex dictates the network geometry. The network is stretched along the ski jumps (Figure 4)

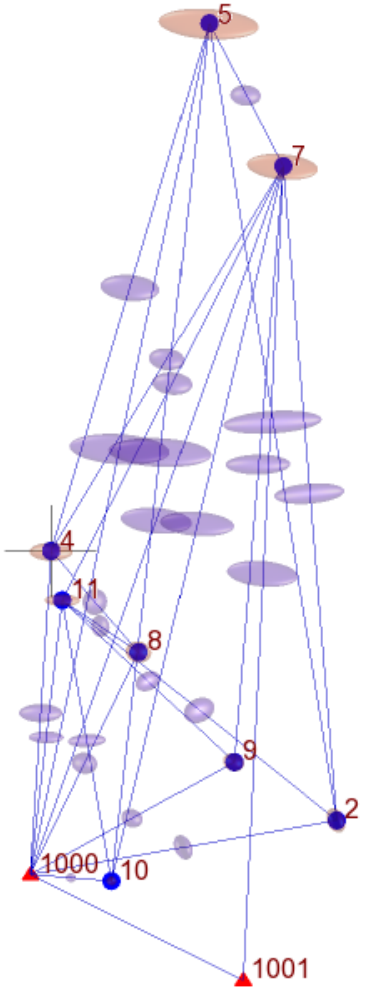

Figure 4. Scheme of the monitoring network.

In Figure 4, apart from the network scheme, the error ellipses are given. The sizes of the error ellipses are presented in Table 1. The network was adjusted using the standard least squares procedure.

Station	Error ellipse parameters			
	Semi-major axis, mm	Semi-minor axis, mm	Azimuth of major axis, deg	Vertical axis, mm
1001	0.000	0.000	0	0.000
1000	0.000	0.000	0	0.000
2	0.005	0,002	176	0.003
4	0.006	0.005	107	0.002
5	0.016	0.003	116	0.002
7	0.012	0.002	120	0.002
8	0.004	0.002	143	0.003
9	0.004	0.003	166	0.002
10	0.002	0.001	117	0.001
11	0.005	0.002	108	0.001

Table 1. Network accuracy.

The lowest accuracy has been obtained for the points located down the ski jump hill. As far as the monitoring of the landing hill needs lower accuracy, the obtained results are considered acceptable. Meanwhile, the points around the ski jump ramps were determined with accuracy that does not affect monitoring results. In what follows, these points were used for scanning stations. It is worth mentioning that for every observation epoch, the network is remeasured, and the appropriate corrections to the point coordinates are applied.

3.3 Scanning Results

The scanning has been accomplished by Leica Nova MS60. The point cloud is not highly-dense and contains 40K – 50K points (Figure 5).

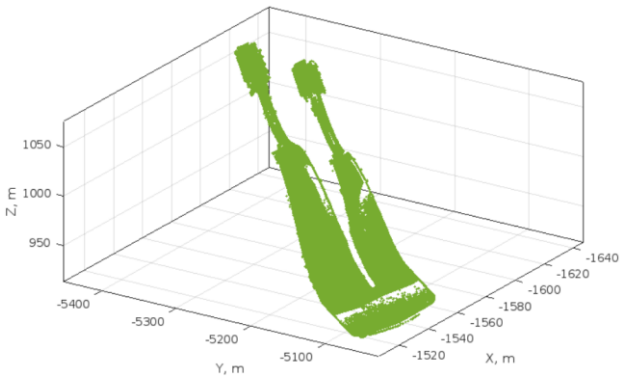

Figure 5. Georeferenced point cloud for two ski jumps.

Two observation epochs were conducted. Since the main interest has the displacements in a vertical direction for the ski jump ramp, it was decided to make cross-sections along the longitude axis. An example of such a cross-section is portrayed in Figure 6.

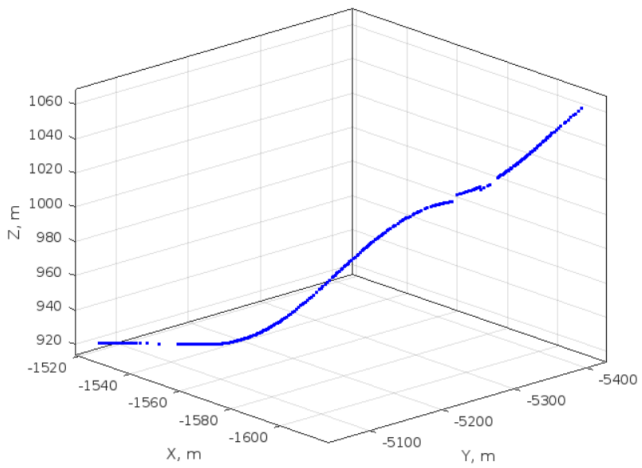

Figure 6. Longitude cross-section.

The cross-section clearly demonstrates the two parts of the ski jump, the upper part corresponds to the ramp, and the bottom part corresponds to the landing hill. As far as the primary goal of the monitoring is the study of the ramp displacements, further analysis has been carried out for the upper part of the ski jump.

4. DISPLACEMENT MODELING

4.1 Spline Functions

The final step of monitoring is displacement modeling. However, for the TLS data, this task becomes a bit tricky. Insofar as the point clouds for the different observation epochs have different distributions and it is impossible to measure the coordinates of the same points, the solution is to apply the interpolation

technique. The strict correspondence between the points in different epochs has to be established for the coordinate comparison. Otherwise, the discrepancies will distort the actual values of the determined displacements. In Figure 7, the case of correspondence search between the design model and TLS point cloud is presented.

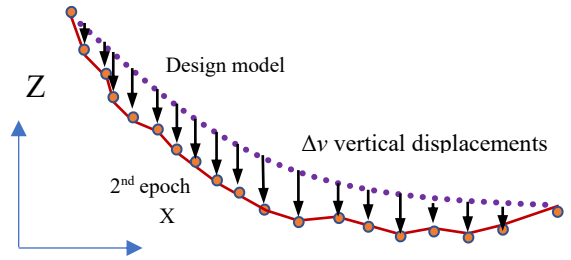

Figure 7. The correspondence between the design model and point cloud.

Therefore, it is necessary to have a definite correspondence between the points in different observation epochs. The straightforward approach is to compare the preliminary marked points, but we only have recognizable points on the ski jump for georeferencing targets. Thus, it has been suggested to apply interpolation techniques to achieve the required results. For the interpolation models, the cubic spline functions were chosen. The splines have become very popular recently thanks to their robustness. There are many applications that one may find, e.g., in (Kermarrec et al. 2017, Kermarrec et al. 2021). Yet no one has pointed out the application of one spline type better than another (Shults et al. 2021). Typical spline expressions for the spatial curve will be

$$\begin{aligned} x_i(t) &= s_{0xi} + s_{1xi}t + s_{2xi}t^2 + s_{3xi}t^3; \\ y_i(t) &= s_{0yi} + s_{1yi}t + s_{2yi}t^2 + s_{3yi}t^3; \\ z_i(t) &= s_{0zi} + s_{1zi}t + s_{2zi}t^2 + s_{3zi}t^3, \end{aligned} \quad (1)$$

where $s_{0xi}, s_{1xi}, s_{2xi}, \dots, s_{0zi}, s_{1zi}, s_{2zi}, s_{3zi}c$ = unknown spline coefficients

t = spline parameter (spatial distance between the points or increments along the coordinate axis)

In our case, these functions are especially useful since they provide a pretty smooth interpolation for the cross-sections without outbreaks (Figure 8).

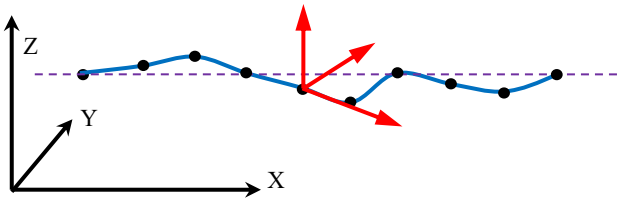

Figure 8. Spline curve is drawn through the set of points.

The different spline functions ensure different interpolation depending on the end conditions, e.g., "Natural" cubic splines, Not-a-knot cubic splines, Hermite splines, modified Hermite splines, B-splines, t-splines, etc. The given study uses the three types of relatively simple cubic splines with cubic, parabolic, and linear end conditions. Visually the difference between these splines is hardly discernible. The modeling has shown that all of the considered spline functions provide similar outputs. The results of interpolation using cubic spline with parabolic end conditions are presented in what follows.

During the monitoring, we obtained the design model of the ski jump complex. It allowed us to generate the ideal cross-section through the center of the ski jump ramp (Figure 9) and further used it for comparison.

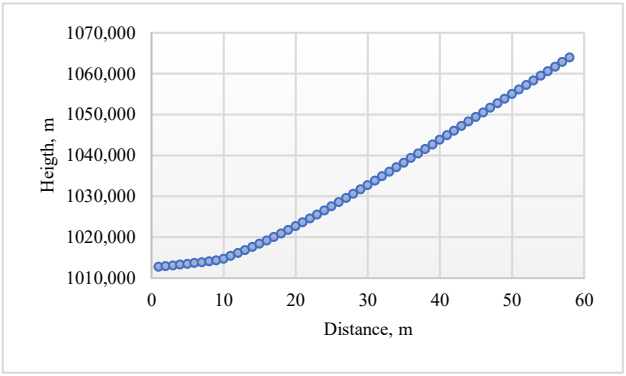

Figure 9. Design cross-section.

The cross-section was generated with 1-meter step. Consequently, the monitoring results were interpolated to get the values for the same points of the design cross-section. Spline interpolation of the TLS data is presented in Figure 10.

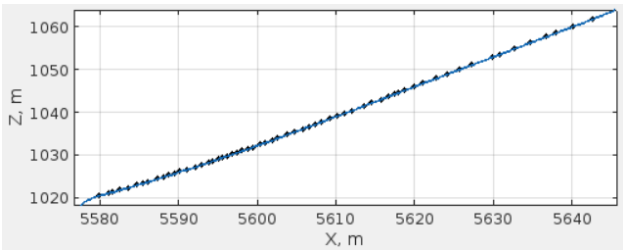

Figure 10. Cubic spline interpolation.

One may see that the points are located unevenly; in turn, we need to interpolate them to find the corresponding points for the design values. Moreover, comparing cross-sections for different observation epochs has the identical drawback. So, the points for the different epochs have to be interpolated too. Having the interpolated values, we may determine the displacements.

4.2 Displacements Modeling

Firstly, the interpolated coordinates of the first epoch were compared with the design values. The differences in coordinates indicate the possible deviation of the ski jump surface as it was built (Figure 11).

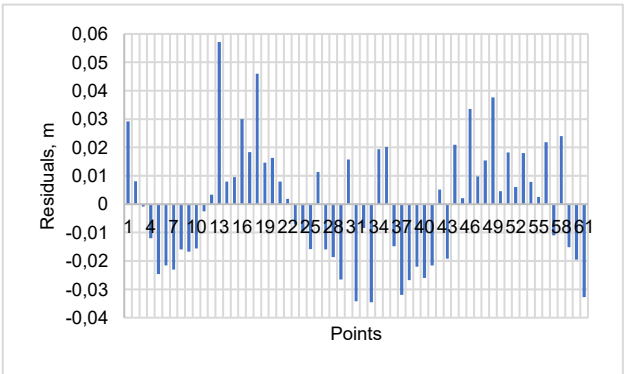

Figure 11. Coordinate differences between the first observation epoch and design values.

The values in Figure 11 provide preliminary evidence that the surface of the K125 ski jump has considerable deviations from the design surface. Apart from some insignificant outliers, all the

rest differences demonstrate periodical dependency. The ski jump surface is waved. These deviations stem from the construction works and indicate the incorrect construction process.

The second observation epoch was accomplished in half a year. The coordinates were interpolated for the same intervals and compared with the first observation epoch. The comparison results are presented in Figure 12.

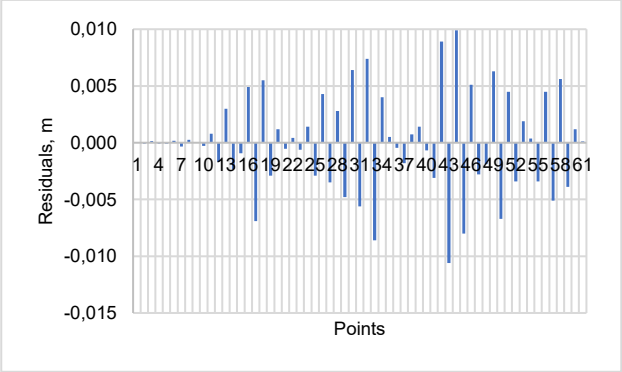

Figure 12. Design model comparison.

These figures suggest that the displacements do not have a place regardless of some values that reach 10 mm. These abnormal values must be treated as blunders or some artifacts on the surface. Contrary to our expectations, the structure is relatively stable and has not undergone any deformations during the observation time.

5. CONCLUSIONS

The presented paper outlines the results of geospatial monitoring of the sports complex 'Sunkar'. The flowchart of the monitoring workflow was developed to carry out the monitoring. The suggested workflow supposes displacement determination differently, i.e., using interpolated point clouds and a design model. As the primary interpolation method, cubic splines were chosen and studied. The study proved the high efficiency of the TLS data for monitoring tasks. However, our findings are not generalizable beyond the scope of this study. Future research will have to confirm whether the suggested workflow is applicable to other similar structures. Our dataset was limited to two observation epochs. Obviously, it is necessary to have at least ten observation epochs to develop prediction models. Therefore, further studies will be focused on the prediction models. Apart from that, in what follows, we are intended to study the surface interpolation models using different spline models.

REFERENCES

Cha, G., Sim, S.-H., Park, S., Oh, T., 2020: Lidar-based bridge displacement estimation using 3d spatial optimization. *Sensors* 20 (24), 7117, doi.org/10.3390/s20247117

Holst, C., Klingbeil, L., Esser, F., Kuhlmann, H., 2017: Using point cloud comparisons for revealing deformations of natural and artificial objects. In Proc. *INGEO 2017 – 7th International Conference on Engineering Surveying*, Lisbon, Portugal, May 18–20, pp. 1-10.

Ioannidis C., Valani A., Georgopoulos A., Tsiligiris E., 2006: 3D model generation for deformation analysis using laser scanning data of a cooling tower. In Proc. *3rd IAG / 12th FIG Symposium*, Baden, May 22-24, 2006.

Kermarrec, G., Alkhatib, H., Neumann, I., 2018: On the sensitivity of the parameters of the intensity-based stochastic model for terrestrial laser scanner. Case study: B-spline approximation. *Sensors* 18 (9), 2964, doi.org/10.3390/s18092964

Kermarrec, G., Schild, N., Hartmann, J., 2021: Fitting terrestrial laser scanner point clouds with t-splines: Local refinement strategy for rigid body motion. *Remote Sensing* 13 (13), 2494, doi.org/10.3390/rs13132494

Koska B., Křemen T., Pospíšil J., Kyrinovič P., Halíčková J., 2008: Monitoring of Lock Chamber Dynamic Deformation. In Proc. *13th FIG Symposium on Deformation Measurement and Analysis*, Lisbon, 12-15 May 12-15, 2008.

Lindenbergh R., Pfeifer N., Rabbani T., 2005: Accuracy analysis of the Leica HDS3000 and feasibility of tunnel deformation monitoring. In Proc. *ISPRS WG III/3 Workshop "Laser scanning 2005", Enschede*, the Netherlands, September 12-14, 2005.

Nguyen, A.C., Weinand, Y., 2020: Displacement study of a large-scale freeform timber plate structure using a total station and a terrestrial laser scanner. *Sensors* 20 (2), 413, doi.org/10.3390/s20020413

Nuttens N., De Wulf A., Bral L., De Wit B., Carlier L., De Ryck M., Stal C., Constales D., De Backer H., 2010: High Resolution Terrestrial Laser Scanning for Tunnel Deformation Measurements. In Proc. *Facing the challenges – building the capacity FIG Congress 2010*, Sydney, Australia 11-16 April 2010.

Qiu D.W., Wu J.G., 2008: Terrestrial laser scanning for deformation monitoring of the thermal pipeline traversed subway tunnel engineering. *Int. Arch. Photogramm. Remote Sens. Spatial Inf. Sci.*, Vol. XXXVII. Part B5, 491-494.

Rashidi, M., Mohammadi, M., Kivi, S.S., Abdolvand, M.M., Truong-Hong, L., Samali, B., 2020: A decade of modern bridge monitoring using terrestrial laser scanning: Review and future directions. *Remote Sensing* 12 (22), 3796, doi.org/10.3390/rs12223796

Schäfer T., Weber T., Kyrinovič P., Zámečniková M., 2004: Deformation Measurement Using Terrestrial Laser Scanning at the Hydropower Station of Gabčíkovo. In Proc. *INGEO 2004 and FIG Regional Central and Eastern European Conference on Engineering Surveying* Bratislava, Slovakia, November 11-13, 2004.

Schneider D., 2006: Terrestrial laser scanning for area based deformation analysis of towers and water damns. In Proc. *3rd IAG / 12th FIG Symposium*, Baden, May 22-24, 2006.

Shults, R., Annenkov, A., Seitkazina, G., Soltabayeva, S., Kozhayev, Z., Khailak, A., Nikitenko, K., Sossa, B., Kulichenko, N., 2021: Analysis of the displacements of pipeline overpasses based on geodetic monitoring results. *Geodesy and Geodynamics* 13 (1), 50 – 71, doi.org/10.1016/j.geog.2021.09.005

Shults, R., Kravchenko, I., Gorkovchuk, D., 2017: Getting a Correct Geometrical Information from TLS Data for Building Constructions Control Surveying. In Proc. *FIG Working Week 2017 Surveying the world of tomorrow - From digitalization to augmented reality* Helsinki, Finland, May 29–June 2, 2017.

Sternberg H., 2006: Deformation Measurements at Historical Buildings with Terrestrial Laser Scanners. *Int. Arch. Photogramm. Remote Sens. Spatial Inf. Sci.*, Volume XXXVI, Part 5.

Tong, X., Liu, X., Chen, P., Liu, S., Luan, K., Li, L., Liu, S., (...), Hong, Z., 2015: Integration of UAV-based photogrammetry and terrestrial laser scanning for the three-dimensional mapping and monitoring of open-pit mine areas. *Remote Sensing* 7 (6), 6635-6662, doi.org/10.3390/rs70606635

Vezočnik, R., Ambrožič, T., Sterle, O., Bilban, G., Pfeifer, N., Stopar, B., 2009: Use of terrestrial laser scanning technology for long term high precision deformation monitoring. *Sensors* 9 (12), 9873-9895, doi.org/10.3390/s91209873

Xu, X., Yang, H., Kargoll, B., 2019: Robust and automatic modeling of tunnel structures based on terrestrial laser scanning measurement. *International Journal of Distributed Sensor Networks* 15 (11), doi.org/10.1177/1550147719884886